

Magnetic Fields and Polarization in the Diffuse Interstellar Medium

Thematic Areas: Planetary Systems Star and Planet Formation
 Formation and Evolution of Compact Objects Cosmology and Fundamental Physics
 Stars and Stellar Evolution Resolved Stellar Populations and their Environments
 Galaxy Evolution Multi-Messenger Astronomy and Astrophysics

Principal Author:

Name: Susan E. Clark
Institution: Institute for Advanced Study
Email: seclark@ias.edu
Phone: 703-973-9634

Co-authors:

Carl Heiles, University of California at Berkeley, heiles@astro.berkeley.edu
Tim Robishaw, Dominion Radio Astrophysical Observatory, tim.robishaw+drao@gmail.com

Abstract:

Magnetism is one of the most important forces on the interstellar medium (ISM), anisotropically regulating the structure and star formation that drive galactic evolution. Recent high dynamic range observations of diffuse gas and molecular clouds have revealed new links between interstellar structures and the ambient magnetic field. ISM morphology encodes rich physical information, but deciphering it requires high-resolution measurements of the magnetic field: linear polarization of starlight and dust emission, and Zeeman splitting. These measure different components of the magnetic field, and crucially, Zeeman splitting is the only way to directly measure the field strength in the ISM. We advocate a statistically meaningful survey of magnetic field strengths using the 21-cm line in absorption, as well as an observational test of the link between structure formation and field strength using the 21-cm line in emission. Finally, we report on the serendipitous discovery of linear polarization of the 21-cm line, which demands both theoretical and observational follow-up.

Related Astro2020 white papers:

Twelve decades: Probing the interstellar medium from kiloparsec to sub-AU scales.

Principal Author: Stinebring

Studying magnetic fields in star formation and the turbulent interstellar medium.

Principal Author: Fissel

1. Introduction

The ‘neutral’ interstellar medium (ISM) is ionized to a small degree, $\sim 10^{-4}$, enough for the gas to be coupled to the magnetic field. Magnetic forces are fully competitive with gravity, turbulent pressure, and cosmic ray pressure in determining gas dynamics. Magnetic forces are anisotropic and are transmitted from the rare electrons to the plentiful neutral Hydrogen (HI) by collisions and cosmic-ray coupling, both of which become ineffective at small length scales and high volume densities (Hennebelle & Falgarone, 2012; McKee & Ostriker, 2007; Stanimirović & Zweibel, 2018). These magnetically-related phenomena not only make the ISM a fascinating entity in itself, but also lead to the multifaceted process of star formation—and, by extension, galactic and cosmological evolution.

2. Observing Magnetic Fields in the ISM

Invisible interstellar magnetic fields are revealed by the linear polarization of starlight and of infrared dust emission, which are produced by magnetically-aligned dust grains; these polarizations trace the orientation of B_{\perp} , the plane-of-the-sky component, but provide no information on magnetic field strength. Zeeman splitting produces circular polarization that provides the magnetic field strength and direction; the splitting is very small compared to the line width, which makes the measurements sensitivity limited.

2.1. Tracing the Magnetic Field with HI Fibers

The neutral ISM is textured by the ambient magnetic field (see Figure 1). Sensitive, high dynamic range observations of the 21-cm line in emission reveal that high aspect ratio (up to 100:1) HI structures (“HI fibers”) thread the diffuse ISM and trace the local magnetic field orientation as probed by optical starlight polarization (Clark et al., 2014) and *Planck* polarized dust emission (Clark et al., 2015; Kalberla et al., 2016). Magnetically aligned fibers are a fairly common feature of HI emission. The HI fibers are preferentially cold neutral medium (CNM; Clark et al., 2014, 2019; Kalberla et al., 2016) and thus bear important similarities to slender, magnetically dominated HI self-absorption structures in the Galactic Plane (McClure-Griffiths et al., 2006).

Information about the magnetic field is thus encoded in the *morphology* of HI emission and absorption. The shape information in the ISM carries important physical meaning, but decoding it requires 1) high dynamic range observations and 2) algorithms for quantifying the spatial information. The recent Galactic Arecibo L-Band Feed Array Survey (GALFA-HI) mapped the 21-cm line with unprecedented dynamic range over the Arecibo sky ($4'$ spatial resolution over 4 sr; Peek et al., 2018). The HI4PI Survey (Ben Bekhti et al., 2016) achieved an all-sky map at $16'$ by combining the Effelsberg-Bonn HI Survey of the northern sky (EBHIS; Winkel et al., 2016) with the Parkes Galactic All-Sky Survey in the south (GASS; McClure-Griffiths et al., 2009). Other diffuse ISM tracers, particularly those that yield direct information on the magnetic field, have not been mapped with comparable resolution. The *Planck* satellite was a major leap forward for far infrared polarimetry, but *Planck* achieved only $\sim 60'$ resolution observations of polarized dust emission in the diffuse ISM (Planck Collaboration, 2019). An all-sky survey of polarized dust emission like the one proposed for the probe class concept PICO (Probe of Inflation and Cosmic Origins; Hanany

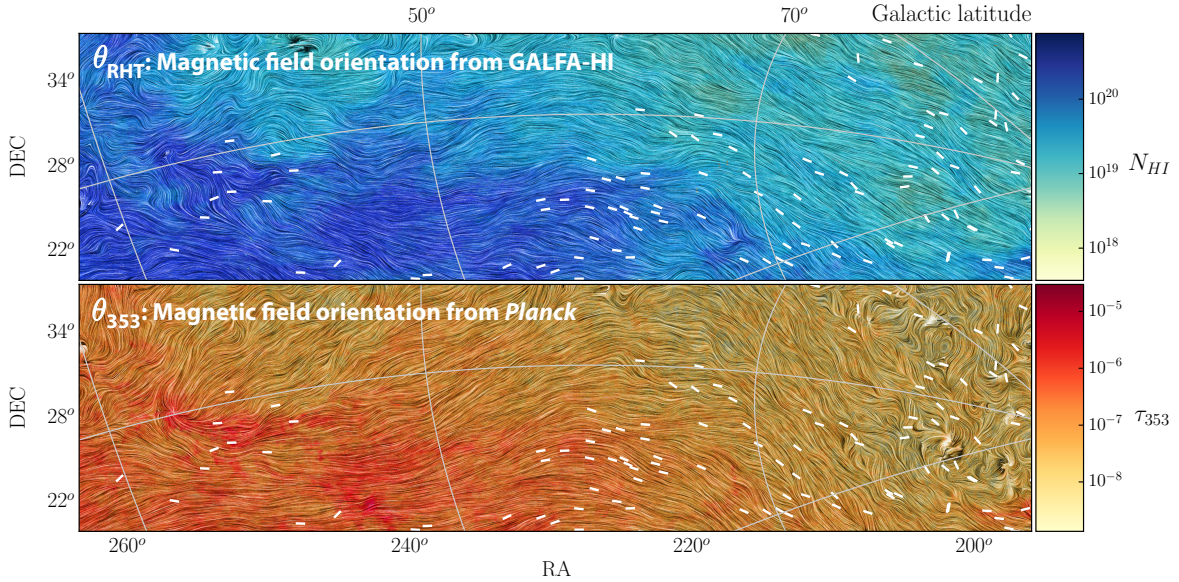


Figure 1: Top: texture shows the orientation of HI structures. Bottom: texture shows the plane-of-sky magnetic field orientation implied from *Planck* 353 GHz polarized emission. White: plane-of-sky magnetic field orientation from optical starlight polarization measurements. Linear HI structures are well aligned with the ambient magnetic field. *Figure reproduced from Clark et al. (2015).*

et al., 2019) would revolutionize the study of magnetic structure in the ISM. The second point—algorithms—is a need for methods that quantify the spatial distribution of emission data. The rich physical information in the morphology of the diffuse ISM mirrors the spectacular advances of the last decade in the study of molecular cloud structure, in which *Herschel* observations revealed that molecular clouds are universally filamentary (Molinari et al., 2010; Arzoumanian et al., 2011; Palmeirim et al., 2013). These observations motivate innovative techniques for quantifying spatial structure in the ISM, and its relationship with the local magnetic field (e.g. Soler et al., 2013).

Disparate observations show an intriguingly similar phenomenon: highly anisotropic, magnetically aligned structures on small scales in the ISM. A striking example in the magneto-ionic medium is the observation of high aspect ratio linear polarization structures with The Low-Frequency Array (LOFAR; Jelić et al., 2015), see Figure 2, left panel. These are straight, and well aligned both with the local magnetic field as probed by polarized dust emission (Zaroubi et al., 2015; Jelić et al., 2018) and with filamentary HI structures (Kalberla & Kerp, 2016). The implication is that the different phases of the ISM know about one another and/or a shared magnetic field. Does this knowledge extend down to the AU-size scales probed by pulsar scintillation (Stinebring et al., 2019)? Are these structures related to a particular geometry, such as the compressed shell of the Local Bubble (e.g. Lallement et al., 2014), or are they a signature of similar diffuse structure formation processes across phases? Parsing the relationship between the magnetic field and the phases of the ISM requires high-resolution observations of magnetic field structure in the molecular gas and neutral medium (Zeeman splitting, polarized dust emission, starlight polarization), as well as the warm ionized medium (Faraday rotated diffuse synchrotron polarization).

The discovery that HI structure carries information about the local magnetic field orientation has tantalizing implications for mapping the magnetic field structure in three dimensions. HI emission is measured in position-position-velocity space: the third dimension available to spectral line observations is not spatial, but the Doppler-shifted emission frequency along the line of sight. With stellar photometry of millions of stars, huge progress has been made recently in mapping dust reddening in three spatial dimensions (Green et al., 2018). With the advent of *Gaia*, the

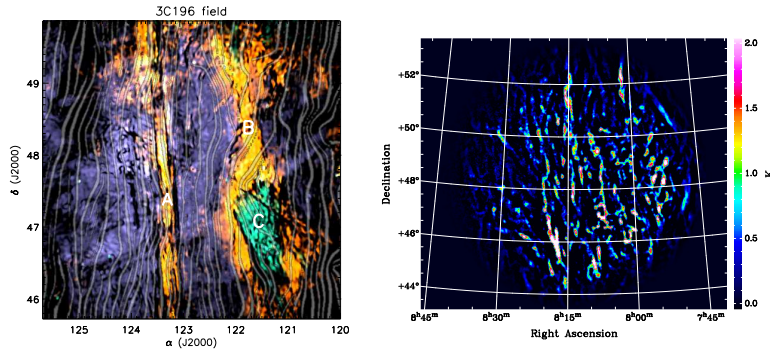


Figure 2: Left: 3C196 field showing distinct features at three different Faraday depths (purple, yellow, green), and *Planck* 353 GHz magnetic field orientation (gray contours). *Figure reproduced from Zaroubi et al. (2015)*. Right: Anisotropic HI structures in the same field. *Figure reproduced from Kalberla & Kerp (2016)*.

accuracy of stellar distance measurements has vastly improved. Still lacking are ample starlight polarization measurements, both in the optical, for studying the diffuse ISM, and in the infrared, for extincted sightlines in the Galactic plane (e.g. GIPS; Clemens et al., 2012). The Polar-Areas Stellar Imaging in Polarization High-Accuracy Experiment will provide a major advance, measuring linear polarization toward millions of stars at high Galactic latitudes (PASIPHAЕ; Tassis et al., 2018). A statistical sample of Zeeman splitting observations (§2.2) would provide the crucial missing component: the magnetic field *strength*.

In addition to being a fascinating physical system in its own right, the diffuse, magnetized ISM is also a formidable foreground for cosmological observations. In particular, the much-sought-after inflationary gravitational wave *B*-mode polarization signal in the cosmic microwave background (CMB) is buried under much brighter polarized Galactic emission at all wavelengths (BICEP2/Keck & Planck Collaborations, 2015; Kogut & Fixsen, 2016). All of the observations discussed here – HI emission structure, diffuse polarized dust emission, starlight polarization data, Zeeman measurements of the magnetic field strength – will aid CMB foreground removal (Tassis & Pavlidou, 2015; Clark, 2018; Hensley & Bull, 2018).

2.2. Building an Unbiased Sample of Magnetic Field Strengths in the CNM Using the HI Line in Absorption

The line-of-sight component of the magnetic field strength ($B_{||}$) in the CNM can be probed via the absorption of continuum emission from compact background sources, which are distributed randomly on the sky. This method was successfully used by Heiles & Troland (2004, 2005) at the Arecibo telescope to make the unprecedented “Millennium” survey of the CNM towards 42 radio-loud sources. The unique products of such observations include not only the field strength, but also accurate kinetic temperatures—and, from the line width, the degree of turbulence and whether it is supersonic and/or super-Alfvénic. This combination of physical properties is essential for understanding the magneto-gas dynamics and can be obtained by no other observational technique.

While these results are important and widely referenced, the number of actual detections is, from a statistical standpoint, pitifully small. The cyan diamonds in the left panel of Figure 3 show the 42 sources. These constitute about 7.5% of the total number of sources within the Arecibo declination range that exceed the minimum useful flux density of 1 Jy. The Arecibo sky contains four important and distinguishable interstellar structures: Perseus, the Orion/Eridanus superbubble, the North Polar Spur superbubble (a.k.a. the Radio Loop 1 superbubble), and the Radio Loop

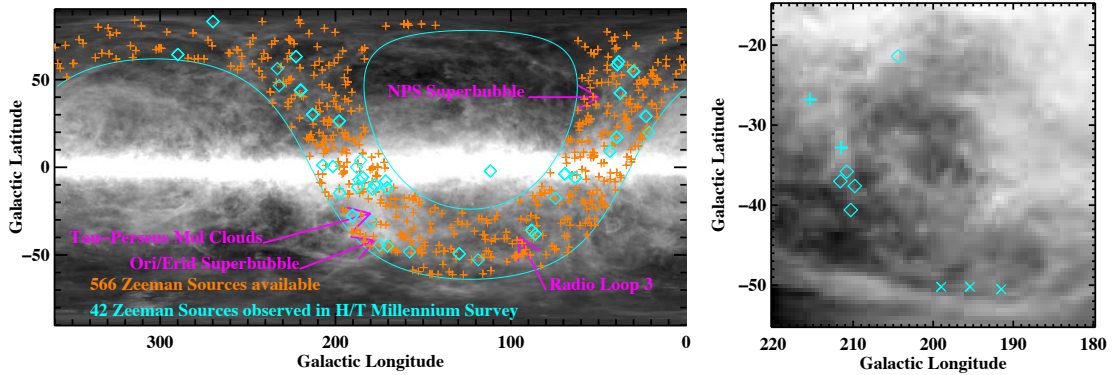


Figure 3: *Left*: the 42 Millennium survey sources (cyan diamonds) and the 566 sources exceeding 1 Jy (orange crosses) within the Arecibo declination range (cyan lines), superposed on a grey-scale image of HI. *Right*: Magnetic field signs from Zeeman splitting of HI emission lines. Pluses are positive, crosses negative, and diamonds are non-detections, superposed on a grey-scale image of the HI line in a portion of the Orion/Eridanus superbubble. $|B_{||}|$ ranges from 4 to 11 μ Gauss.

3 superbubble. Each of these entities is sampled by only a handful of sources. This is simply inadequate to develop a statistically reliable picture of the magnetic field and its fluctuation within each structure.

2.3. Sampling Magnetic Field Strengths in Shocks and Filaments Using the HI Line in Emission

Heiles (1989) measured Zeeman splitting of Galactic HI in emission, targeting compressed super-shell walls and filaments. Figure 3 (right panel) shows the results for a portion of the Orion/Eridanus superbubble. Three things stand out from this image: 1. The HI is swept up from the interior into shell walls, which themselves have considerable spatial structure that sometimes looks filamentary. 2. The observational sampling is totally inadequate relative to the structural details of the HI. 3. There is an apparent large-scale field reversal across the superbubble. However, the sampling is so coarse that no statistically firm statement about field reversal can be made—at *any* scale.

The advantage of emission over absorption measurements is that one can choose interesting positions based on ISM structure; one is not limited to the arbitrary positions of background continuum sources. Heiles (1989) sampled 73 positions in superbubble walls, which are compressed by shocks, and found that the measured field strengths are about twice those of the randomly-selected positions of §2.2. These emission measurements were all made with the Hat Creek 85-foot telescope, which collapsed during a major windstorm in January 1993. Robishaw and Heiles are initiating collaborative development of instrumentation and techniques for the DRAO Galt 26-m, the Parkes 64-m, and the Effelsberg 100-m telescopes to expand the coverage of emission measurements.

3. A Serendipitous Discovery: Linear Polarization of the 21-cm Line

For technical reasons we wanted to observe a set of test sources known to be unpolarized. We expected the 21-cm line to be unpolarized because its 2 level system is populated overwhelmingly by collisions. We used the Heiles & Troland Millennium survey (2003) data because of their long integration times and careful polarization calibration. We studied a subset of 18 sources and

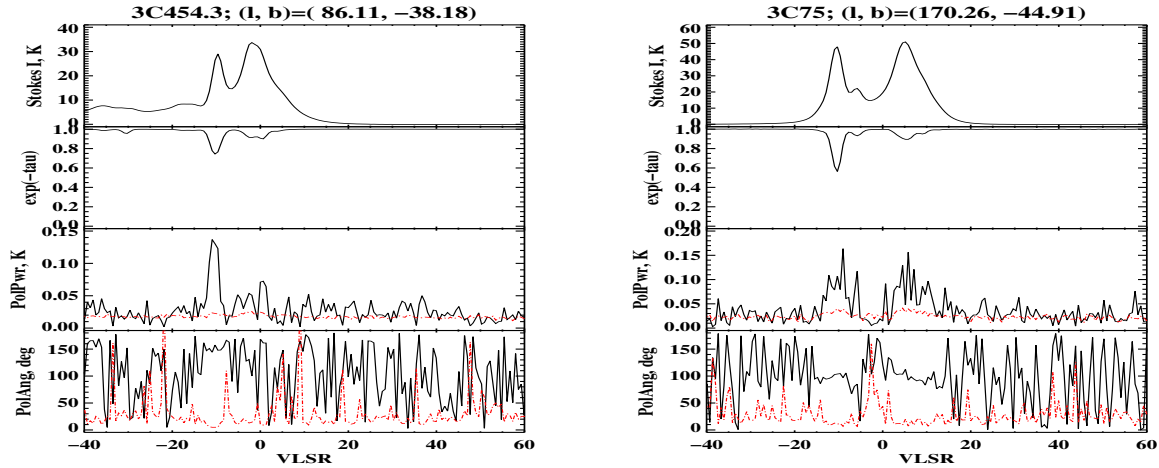


Figure 4: Each of the four panels shows: top, Stokes I emission spectrum; next, the optical depth spectrum $\exp(-\tau)$; next, the total linear polarization power $(Q^2 + U^2)^{1/2}$; bottom, the position angle of linear polarization $\frac{1}{2}\text{atan}(Q/U)$. The solid (black) line is the spectral quantity and the red (dashed) line its statistical uncertainty.

found, much to our surprise, that 13 of these 18 sources exhibit detectable linear polarization at levels 0.14% to 0.35%. The linear polarization appears to be astrophysical, and we are currently exerting considerable effort to confirm or refute the finding.

Figure 4 shows two examples, 3C75 and 3C454.3. The top panel exhibits the emission line and the absorption line. The bottom panels exhibit the linearly polarized power and the position angle; the black lines are the profiles and the red their uncertainties. Figure 4 shows that the polarization is not exclusively associated with either the absorption profiles (the CNM) or the emission profiles (both the warm neutral medium and the CNM). How can the collisionally-dominated two-level system show linear polarization? While we idealize the hyperfine levels of the H I atom as a two-level system, this is not strictly true. Ly- α radiation is an important populating agent for the 21-cm levels (Murray et al., 2014), and could conceivably differentially populate the magnetic sublevels, particularly if it is anisotropic in either physical or frequency space. Indeed, we were surprised to learn that linear polarization of the 21-cm line was predicted by Yan & Lazarian (2007). We speculate that the spatial anisotropies of §2.1 are involved with the 21-cm line polarization.

4. Instrumental Requirements for §2.2 and §3

Measuring circular polarization (§2.2) and linear polarization (§3) requires obtaining not only the four on-source HI Stokes parameter spectra, but also the emission spectra that would be observed if the source were absent. This requires sensitive and accurate measurements of the HI profile, which can only be done with a large single dish telescope; interferometric arrays cannot measure the spatially extended emission spectra with high sensitivity. Arecibo could supply more than 500 additional sources for the expenditure of ~ 3000 hours of telescope time using its new phased-array ALPACA feed, which allows 39 off-source emission spectra and the on-source spectrum to be measured simultaneously (Cortes-Medellin et al., 2016).

The next decade is poised to dramatically advance our understanding of interstellar magnetism, one of the primary forces acting on the Galaxy. This will be achieved with an investment in polarimetry: surveys of polarized dust emission, starlight polarization, and single-dish measurements of Zeeman splitting.

References

- Arzoumanian, D., André, P., Didelon, P., Könyves, V., Schneider, N., Men'shchikov, A., Sousbie, T., Zavagno, A., Bontemps, S., di Francesco, J., Griffin, M., Hennemann, M., Hill, T., Kirk, J., Martin, P., Minier, V., Molinari, S., Motte, F., Peretto, N., Pezzuto, S., Spinoglio, L., Ward-Thompson, D., White, G., & Wilson, C. D. 2011, *A&A*, 529, L6
- Ben Bekhti, N., Flöer, L., Keller, R., Kerp, J., Lenz, D., Winkel, B., Bailin, J., Calabretta, M. R., Dedes, L., Ford, H. A., Gibson, B. K., Haud, U., Janowiecki, S., Kalberla, P. M. W., Lockman, F. J., McClure-Griffiths, N. M., Murphy, T., Nakanishi, H., Pisano, D. J. & Staveley-Smith, L. 2016, *A&A*, 594, 116
- BICEP2/Keck Collaboration & Planck Collaboration. 2015, *Phys. Rev. Lett.*, 114, 101301
- Clark, S. E., Peek, J. E. G., & Putman, M. E. 2014, *ApJ*, 789, 82
- Clark, S. E., Hill, J. C., Peek, J. E. G., Putman, M. E., & Babler, B.L. 2015, *Phys. Rev. Lett.*, 115, 241302
- Clark, S. E. 2018, *ApJ*, 857, L10
- Clark, S. E., Peek, J. E. G., & Miville-Deschênes, M.-A. 2019, accepted to *ApJ*, arXiv:1902.01409
- Clemens, D. P., Pinnick, A. F., Pavel, M. D. & Taylor, B. W. 2012, *ApJS*, 200, 19
- Cortes-Medellin, G., Parshley, S., Campbell, D. B., Warnick, K. F., Jeffs, B. D. & Ganesh, R. 2016, *Proc. SPIE*, 9908, 5
- Green, G. M., Schlafly, E. F., Finkbeiner, D., Rix, H.-W., Martin, N., Burgett, W., Draper, P. W., Flewelling, H., Hodapp, K., Kaiser, N., Kudritzki, R.-P., Magnier, E. A., Metcalfe, N., Tonry, J. L., Wainscoat, R. & Waters, C. 2018, *MNRAS*, 478, 651
- Hanany, S., Alvarez, M., Artis, E., Ashton, P., Aumont, J. et al. 2019, Probe class mission study submitted to NASA and 2020 Decadal Panel. arXiv:1902.10541
- Heiles, C. 1989, *ApJ*, 336, 808
- Heiles, C. & Troland, T.H. 2003, *ApJS* 145, 329
- . 2004, *ApJS*, 151, 271
- . 2005, *ApJ*, 624, 773
- Hennebelle, P., & Falgarone, E. 2012, *ARA&A*, 20, 55
- Hensley, B. S. and Bull, P. 2018, *ApJ*, 853, 127
- Jelić, V., de Bruyn, A. G., Pandey, V.N., Mevius, M. et al. *A&A*, 583, A137
- Jelić, V., Prelogović, D., Haverkorn, M., Remeijn, J. & Klindžić, D. 2018, *A&A*, 615, L3
- Kalberla, P. M. W., Kerp, J., Haud, U., Winkel, B., Ben Bekhti, N., Flöer, L. & Lenz, D. 2016, *ApJ*, 821, 117
- Kalberla, P. M. W. & Kerp, J. 2016, *A&A*, 595, 37K
- Kalberla, P. M. W., Kerp, J., Haud, U. & Haverkorn, M. *A&A*, 607, A15
- Kogut, A. & Fixsen, D. J. 2016, *ApJ*, 826, 101
- Lallement, R., Vergely, J.-L., Valette, B., Puspitarini, L., Eyer, L. & Casagrande, L. 2014, *A&A*, 561, 91
- McClure-Griffiths, N. M., Dickey, J. M., Gaensler, B. M., Green, A. J. & Haverkorn, M. 2006, *ApJ*, 652, 1339
- McClure-Griffiths, N. M., Pisano, D. J., Calabretta, M. R., Ford, H. A., Lockman, F. J., Staveley-Smith, L., Kalberla, P. M. W., Bailin, J., Dedes, L., Janowiecki, S., Gibson, B. K., Murphy, T., Nakanishi, H. & Newton-McGee, K. 2009, *ApJS*, 181, 398
- McKee, C. F. & Ostriker, E. C. 2007 *ARA&A*, 45, 565
- Molinari, S., Swinyard, B., Bally, J., Barlow, M., Bernard, J.-P., Martin, P., Moore, T., Noriega-Crespo, A. et al. 2010, *A&A*, 518, L100
- Murray, C., Lindner, R.R., Stanimirović, S. Goss, W.M., Heiles, C., Dickey, J., Pingel, N.M., Lawrence, A., Jencson, J., Babler, B.L., Hennebelle, P., 2014, *ApJ*, 781, L41
- Palmeirim, P., André, P., Kirk, J., Ward-Thompson, D., Arzoumanian, D., Könyves, V., Didelon, P., Schneider, N., Benedettini, M., Bontemps, S., Di Francesco, J., Elia, D., Griffin, M., Hennemann, M., Hill, T., Martin, P. G., Men'shchikov, A., Molinari, S., Motte, F., Nguyen Luong, Q., Nutter, D., Peretto, N., Pezzuto, S., Roy, A., Rygl, K. L. J., Spinoglio, L. & White, G. L. 2013, *A&A*, 550, 38
- Peek, J. E. G., Babler, B. L., Zheng, Y., Clark, S. E., Douglas, K. A., Korpela, E. J., Putman, M. E., Stanimirović, S., Gibson, S. J. & Heiles, C. 2018, *ApJS*, 234, 2
- Planck Collaboration. 2019, accepted to *A&A*, arXiv:1807.06212
- Soler, J. D., Hennebelle, P., Martin, P. G., Miville-Deschênes, M.-A., Netterfield, C. B. & Fissel, L. M. 2013, *ApJ*, 774, 128
- Stanimirović, S. & Zweibel, E. G. 2018 *ARA&A*, 56, 489
- Stinebring, D. et al. 2019, *Astro2020 white paper: "Twelve Decades: Probing the interstellar medium from kiloparsec to sub-AU scales"*
- Tassis, Konstantinos, Ramaprakash, Anamparambu N., Readhead, Anthony C. S., Potter, Stephen B., Wehus, Ingunn K., Panopoulou, Georgia V., Blinov, Dmitry, Eriksen, Hans Kristian, Hensley, Brandon, Karacki, Ata, Kypriotakis, John A., Maharana, Siddharth, Ntormousi, Evangelia, Pavlidou, Vasiliki, Pearson, Timothy J. & Skalidis, Raphael. 2018, arXiv:1810.05652
- Tassis, K. & Pavlidou, V. 2015, *MNRAS*, 451, L90
- Yan, H. & Lazarian, A. 2007, *ApJ*, 657, 618
- Winkel, B., Kerp, J., Flöer, L., Kalberla, P. M. W., Ben Bekhti, N., Keller, R. & Lenz, D. 2016, *A&A*, 585, A41
- Zaroubi, S., Jelić, V., de Bruyn, A. G., Boulanger, F., Bracco, A., Kooistra, R., Alves, M. I. R., Brentjens, M. A., Ferrière, K., Ghosh, T., Koopmans, L. V. E., Levrier, F., Miville-Deschênes, M.-A., Montier, L., Pandey, V. N. & Soler, J. D. 2015, *MNRAS*, 454, L46